


Pixel-by-pixel precise delay correction for measurement of cerebral hemodynamic parameters in $H_2^{15}O$ PET study

Muhammad M. Islam¹ · Tetsuya Tsujikawa¹ · Tetsuya Mori¹ · Yasushi Kiyono¹ · Hidehiko Okazawa¹ 

Received: 22 January 2017 / Accepted: 30 January 2017 / Published online: 27 February 2017
© The Author(s) 2017. This article is published with open access at Springerlink.com

Abstract

Objective A new method of delay time estimation was proposed to measure precise cerebral blood flow (CBF) and arterial-to-capillary blood volume (V_0) using ^{15}O -water PET.

Methods Nineteen patients with unilateral arterial stenocclusive lesions were studied to evaluate hemodynamic status before treatment. The delay time of each pixel was calculated using least squares fitting with an arterial blood input curve adjusted to the internal carotid artery counts at the skull base. Pixel-by-pixel delay estimation provided a delay map image that could be used for precise calculation of CBF and V_0 using a one-tissue compartment model, and the values from this method were compared with those from the slice-by-slice correction method.

Results The affected side showed a longer delay time than the contralateral cerebral hemisphere. Although the mean cortical CBF values were not different between the two methods, the slice-by-slice delay correction overestimated CBF in the hypo perfused area. The scatter plot of V_0 pixel values showed significant difference between the two correction methods where the slice-by-slice delay correction significantly overestimated V_0 in the whole brain ($P < 0.05$).

Conclusion Pixel-by-pixel delay correction provides delay images as well as better estimation of CBF and V_0 , thus offering useful and beneficial information for the treatment of cerebrovascular disease.

Keywords $H_2^{15}O$ PET · Delay correction · Pixelwise calculation · Cerebral blood flow · Arterial-to-capillary blood volume (V_0)

Introduction

Precise measurements of cerebral blood flow (CBF) and other hemodynamic parameters are important in the diagnosis of impaired status in cerebrovascular diseases (CVD). For the quantitative measurement of these parameters using positron emission tomography (PET) and ^{15}O -labeled tracers, the steady-state and autoradiographic (ARG) methods based on a single compartment model were proposed to evaluate cerebral hemodynamics [1–4]. A one-tissue compartment model (1-TCM) was applied as the next step, to obtain more precise values of CBF using a better kinetic description for avoiding effects of radioactivity in the vessels and the distribution of water into brain tissues [5–7].

Quantitative values of hemodynamic parameters in the ^{15}O -PET with arterial blood sampling are affected by the accuracy of an input function corrected for parameters such as tracer delay time and dispersion constants [4, 8]. The precision of CBF and arterial-to-capillary blood volume (V_0) calculation with a 1-TCM was reported to be sensitive to the delay correction, i.e., the difference between tracer arrival times at brain tissue and the arterial sampling site [6, 9]. To simplify the model parameter estimation and calculate efficiently using the 1-TCM, programs employed a fixed dispersion constant and a single delay time for the whole brain, or slice-by-slice delay correction was applied [6, 7, 9]. However, correction parameters for the whole brain or for each brain slice may cause errors in calculation of hemodynamic parameters because the values could

✉ Hidehiko Okazawa
okazawa@u-fukui.ac.jp

¹ Biomedical Imaging Research Center, University of Fukui, 23-3, Matsuoka-Shimaizuki, Eiheiji-cho, Fukui 910-1193, Japan

be affected by estimation errors of delay and dispersion of the arterial input.

Delay time estimation is not so simple because it varies according to the brain structure and arterial distribution or collaterals that supply regional blood flow [10–12]. Furthermore, since the brain is a heterogeneous mixture of gray and white matter with different amounts of blood flow, each voxel in the brain requires a unique delay and dispersion correction for ^{15}O -tracer arrival even within the same slice [2, 4, 13]. Patients with unilateral arterial stenocclusive lesions would have different delays in each hemisphere [14, 15]; however, slice-by-slice adjustment of the delay correction applies a single input function corrected for delay and dispersion time to all pixels in the same slice level despite different tracer arrival times for each pixel in the slice, which may not reflect appropriate CBF and V_0 values over the entire brain because of substantial biases in regional delay estimation [14].

This study was designed to evaluate the effects of delay time correction by pixel-by-pixel estimation for precise measurements of hemodynamic parameters such as CBF and V_0 with a 1-TCM [6, 7]. The CBF and V_0 values from this new correction method were compared with those obtained from the standard method using slice-by-slice delay correction [7, 11].

Materials and methods

Subjects

Nineteen patients (18 males and 1 female, mean age = 68.8 ± 9.8 y.o.) with unilateral stenocclusive disease in the major cerebral arteries were included in the study. Twelve patients had stenosis and five patients had occlusions in the unilateral internal carotid artery (ICA), one had a middle cerebral artery (MCA) occlusion, and the other had a common carotid artery occlusion. Ten patients had transient or minor persistent symptoms of transient ischemic attack (TIA), probably due to stenocclusive CVD, and seven of them had lacunar infarctions on MRI. The other nine patients were asymptomatic. They underwent a ^{15}O -PET study to evaluate their hemodynamic status before deciding on further treatment because the Japanese Guidelines for the Management of Stroke published by the Japan Stroke Society recommends PET or SPECT studies to detect regions of severely impaired cerebral hemodynamics before extracranial–intracranial (EC–IC) bypass surgery or other neurosurgical treatments. The PET study was approved by the Ethics Committee of our institute, and written informed consent was obtained from each patient. This study was designed retrospectively to improve

accuracy of hemodynamic PET parameters using the ^{15}O -PET data.

PET data acquisition

A whole-body PET scanner (Advance, GE Medical Systems, Milwaukee, WI, USA) was used for PET data acquisition. The scanner permits simultaneous acquisition of 35 image slices in 2-dimensional mode with an interslice spacing of 4.25 mm [16]. Performance tests showed the intrinsic resolution of the scanner to be 4.6–5.7 mm in the transaxial direction and 4.0–5.3 mm in the axial direction. The PET data were reconstructed using a Hanning filter with a resolution of 5.0 mm full-width at half-maximum in the transaxial direction and a 128×128 matrix in $2 \times 2 \times 4.25$ mm voxel size. Patients were positioned on the scanner bed with their heads immobilized using a head holder. A small cannula was placed in the right brachial artery for blood sampling. A 10-min transmission scan was acquired before the emission scan with a $^{68}\text{Ge}/^{68}\text{Ga}$ rod source for attenuation correction. ^{15}O -water and ^{15}O -gas ($^{15}\text{O}_2$ and C^{15}O) PET studies were performed with arterial blood sampling. Details of the protocol have been described previously [17, 18]. In brief, each subject first inhaled a single dose of C^{15}O (1000 MBq) to obtain a cerebral blood volume (CBV) image (mL/100 g). Arterial blood was sampled twice during a 3-min static C^{15}O -PET scan started about 50 s after the slow inhalation of C^{15}O . Ten minutes after the C^{15}O scan, a 3-min static PET acquisition was started with a slow bolus inhalation of $^{15}\text{O}_2$ (1000 MBq) to obtain images of the oxygen extraction fraction (OEF) and cerebral metabolic rate of oxygen (CMRO_2) (mL/100 g/min) using the ARG method [19].

Finally, two scans of 3-min dynamic PET acquisition with a bolus injection of 555 MBq ^{15}O -water were performed to calculate CBF (mL/100 g/min) images before and 10 min after administration of acetazolamide (ACZ) (1.0 g/60 kg BW). Each dynamic scan consisted of $2 \text{ s} \times 30$, $10 \text{ s} \times 6$, and $20 \text{ s} \times 3$ frames. Radioactivity in the arterial blood during $^{15}\text{O}_2$ and H_2^{15}O scans was counted by an automatic arterial blood sampling system (ABSS), consisting of a positron radioactivity counter (Apollomec Co. Ltd., Kobe, Japan) and a mini-pump (AC-2120, Atto Co., Tokyo, Japan). Arterial blood was sampled and counted continuously at a constant rate of 7 mL/min for the first 2 min using the ABSS, followed by manual sampling of 0.5 mL of blood every 20 s during the remaining scan time. Radioactivity, as counted by the ABSS, was calibrated with the manually sampled blood at 2 min after tracer administration. Decay of the radioactivity from dynamic PET acquisition and blood data was corrected to the starting point of each scan. The arterial input function from ABSS thus obtained was corrected for dispersion of the external

tube in the ABSS described previously [20, 21]. Physiological data such as mean blood pressure, arterial pCO₂, pO₂ and O₂c were measured before and after the ACZ injection to confirm stability of each patient’s condition during the scans.

Correction of input function

Dynamic data from each H₂¹⁵O PET scan were used for delay correction of the arterial input function at slice-by-slice and pixel-by-pixel level. In the pixel-by-pixel delay correction method, the time difference between the arterial blood sampling point and local brain tissue pixels was estimated in two steps (Fig. 1). First, the time-activity curves (TAC) from arterial blood sampling with external dispersion correction (TAC_{a1}) was adjusted to that of the cavernous part of ICA obtained from dynamic PET data (TAC_{CA}). The position of the region of interest (ROI) for the TAC_{CA} was determined using the CBV image (Fig. 2). The maximum count in the ROI of each frame was used for the TAC_{CA}. The delay time between the TAC_{a1} and TAC_{CA} was estimated using the slope method except for a few cases whose TACs could not be adjusted by the slope method; the least squares fitting approach was applied in these cases [4, 9, 22]. For delay and dispersion correction of the TAC_{a1}, the same time constant estimated above was used and the TAC_{a2} was obtained [22, 23].

Second, the delay time of tracer arrival at regional brain tissue from the ICA trunk was estimated for each pixel

using the brain pixel TAC (TAC_{bp}) and the TAC_{a2}. The pixel delay time was determined using least-squares fitting for the initial 60 s of TAC_{a2} and TAC_{bp} with a step size of 0.1 s [9], and a delay image was obtained from the pixelwise delay time estimation. As the delay and dispersion constants are very closely correlated [22, 23], the pixel delay time estimated from TAC_{a2} and TAC_{bp} was also used as the dispersion time constant for the TAC_{a2} correction to obtain the local input function. The local input function (C_a), corrected for pixelwise delay and dispersion, was used in the subsequent image calculations.

Calculation of regional CBF and V₀

The model for the 1-TCM can be represented by the following equation [6, 7],

$$\frac{dM_e(t)}{dt} = K_1 C_a(t) - k_2 M_e(t), \tag{1}$$

where M_e(t) (Bq/100 g) is the radioactivity in the brain tissue and C_a(t) (Bq/mL) is the true arterial input function. K₁ (mL/100 g/min) and k₂ (1/min) are the rate constants for influx and outflux of the tracer, respectively [7]. K₁ apparently represents regional CBF. The equation is solved as

$$M_e(t) = K_1 C_a(t) \otimes e^{(-k_2 t)}, \tag{2}$$

where ⊗ represents the convolution. Including the radioactivity in the intravascular spaces, total radioactivity in the brain is expressed as

Fig. 1 In the slice-by-slice correction method, TAC_{a1} is used for CBF calculation after slice-wise delay correction and fixed dispersion (4 s). In the pixel-by-pixel correction method, TAC_{a1} is adjusted to TAC_{CA} (=TAC_{a2}) and brain pixel TAC (TAC_{bp}) was used for delay and dispersion correction of TAC_{a2}. The standard method for delay estimation is slicewise correction or a single delay correction for the whole brain (left flow)

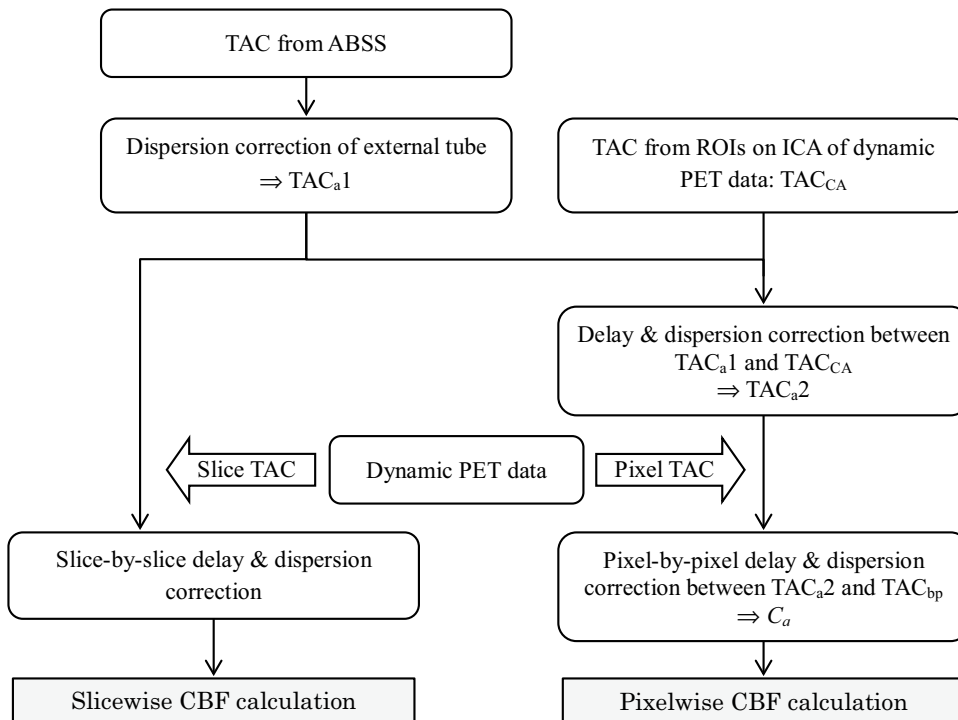
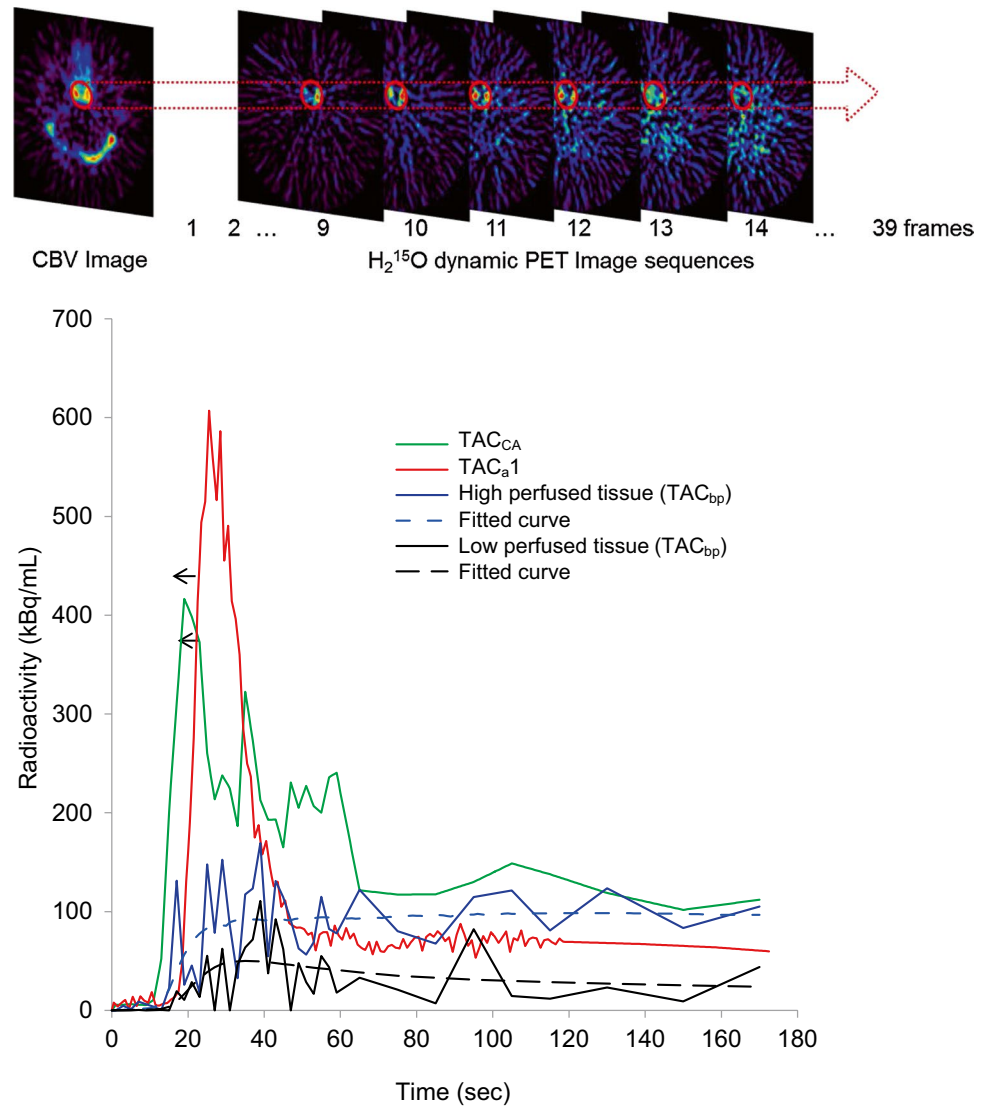


Fig. 2 Upper Scheme showing the region of interest (ROI) for ICA TAC and its application to the dynamic PET data. Bottom Representative TACs from arterial blood sampling (TAC_{a1} , red line), ROI peak value in the ICA region (TAC_{CA} , green line) and the regional pixel value in the high and low perfused brain tissue (TAC_{bp} , blue and black solid lines, respectively). Blue and black dotted lines (fitted curve) show a result of non-linear least squares fitting of the arterial input after delay and dispersion correction for each TAC_{bp} . The arrow shows the direction of delay correction to adjust the initial slope of TAC_{a1} to TAC_{CA} . In cases of a long delay time, the difference between TAC_{a1} and TAC_{CA} was greater than 10 s



$$M(t) = K_1 C_a(t) \otimes e^{-k_2 t} + V_0 C_a(t), \tag{3}$$

where $M(t)$ (Bq/100 g) is the regional PET count, and V_0 (mL/100 g) is the arterial-to-capillary vascular volume [7]. Here, K_1 , k_2 and V_0 can be calculated from measured $M(t)$ and $C_a(t)$ using the weighted method to reduce the image calculation time [6, 7, 12]. In brief, Eq. 3 can be integrated after weighting with three different weights of $w_i(t)$ ($i=1-3$) as below:

$$\int_0^T w_i(t)M(t)dt = K_1 \int_0^T w_i(t)C_a(t) \otimes e^{-k_2 t} dt + V_0 \int_0^T w_i(t)C_a(t)dt, \tag{4}$$

Equation 5 is obtained by rearranging three equations of Eq. 4 to eliminate the V_0 term, where K_1 is cancelled, and various k_2 values can be estimated from the right-hand side ratio using the table look-up method.

$$\frac{\int_0^T w_3(t)C_a(t)dt \times \int_0^T w_1(t)M(t)dt - \int_0^T w_1(t)C_a(t)dt \times \int_0^T w_3(t)M(t)dt}{\int_0^T w_3(t)C_a(t)dt \times \int_0^T w_2(t)M(t)dt - \int_0^T w_2(t)C_a(t)dt \times \int_0^T w_3(t)M(t)dt} = \frac{\left[\int_0^T w_3(t)C_a(t)dt \times \int_0^T w_1(t)C_a(t) \otimes e^{k_2 t} dt - \int_0^T w_1(t)C_a(t)dt \times \int_0^T w_3(t)C_a(t) \otimes e^{k_2 t} dt \right]}{K_1 \left[\int_0^T w_3(t)C_a(t)dt \times \int_0^T w_2(t)C_a(t) \otimes e^{k_2 t} dt - \int_0^T w_2(t)C_a(t)dt \times \int_0^T w_3(t)C_a(t) \otimes e^{k_2 t} dt \right]}. \tag{5}$$

The K_1 values can be estimated either from the numerator or denominator by substituting the k_2 values in Eq. 5. The same weighting functions of $w_1(t)$ to $w_3(t)$ were used as in the original papers [6, 7]. Finally, the parameter V_0 can be obtained from K_1 and k_2 using Eq. 4 [6].

Details of the slice-by-slice calculation method are described elsewhere [6, 7, 22, 23]. In brief, a single delay time estimated from the mean TAC of each slice of the brain was used in the calculation program based on Eqs. 4

and 5 with fixed dispersion of 4 s (Fig. 1). A MATLAB toolkit included in the EMMA (Extensible MATLAB Medical image Analysis: <http://www.bic.mni.mcgill.ca/software/emma/>) programs developed at the Montreal Neurological Institute (McGill University, Montreal, Canada) was modified and applied for the calculation of the weighted integration method. In the pixel-by-pixel calculation, pixelwise correction for delay and dispersion of the arterial input function was applied to measurement of CBF and V_0 (Fig. 1). The programs for the pixel-by-pixel were modified from the slice-by-slice calculation described above. An individual mask image to exclude radioactivity outside of the brain obtained from the average tissue activity image was applied to the dynamic PET data before CBF and V_0 calculation to reduce the calculation time. The final parametric PET images were smoothed using a Gaussian filter with a size of 6 mm.

Cerebral vascular reactivity (CVR) was calculated as the percentage change in CBF from images before and after the ACZ challenge test for both slice-by-slice (CVR_s) and pixel-by-pixel (CVR_p) delay correction.

Error analyses in CBF and V_0 calculation

Error analyses were performed to investigate the biases of the CBF and V_0 estimations with simulated delay time shifts. Several small ROIs 10-mm in diameter, including about 30 voxels, were drawn on the brain cortex of parametric images for various values of CBF (30–70 mL/min/100 g) and V_0 (0.3–2.0 mL/100 g) to obtain tissue TACs from dynamic PET data. The arterial input function after the delay and dispersion correction for the brain tissue TAC ($=C_a$) was shifted from –3 to 3 s in steps of 0.5 s in the analyses. Using these two TACs of tissue activity and shifted C_a , CBF and V_0 were recalculated based on

a 1-TCM. Percent changes from the original CBF and V_0 values were calculated and plotted to observe the effect of delay estimation errors on parametric values.

Statistical analysis

In the MCA territory, 30 circular ROIs 10 mm in diameter were set for each hemisphere. The same ROIs were applied to all parametric images of individual subjects. For statistical analysis, the SPSS ver. 18 (IBM Co., Armonk, NY, USA) was used. Repeated measures analysis of variance (ANOVA) with a post-hoc test by the Student–Newman–Keuls method was applied to analyze the difference in estimated hemodynamic parameters between ipsilateral and contralateral sides, as well as CBF and V_0 values before and after ACZ administration. CBF and V_0 values from the different delay correction methods were also compared. $P < 0.05$ was considered to be statistically significant. Correlation analyses were conducted among different PET parameters from this study to observe relationships as well as to confirm theoretical changes in cerebral hemodynamics.

Results

Representative TACs from arterial blood sampling with dispersion correction for the external tube (TAC_{a1}), maximum ROI values in the ICA region (TAC_{CA}), and one of the pixels in the brain tissue (TAC_{bp}) from both high and low perfused regions are given in Fig. 2. After TAC_{a2} was estimated by delay and dispersion correction of TAC_{a1}, the true input function at each pixel level (C_a) was obtained by delay and dispersion correction of TAC_{a2}. The result of

Table 1 Hemodynamic parameters of ¹⁵O-PET study in patients

Parameter	Ipsilateral		Contralateral	
	Slice-by-slice	Pixel-by-pixel	Slice-by-slice	Pixel-by-pixel
CBF _B (mL/100 g/min)	45.1 ± 6.4*	46.5 ± 7.3*	50.6 ± 5.6	52.6 ± 6.8
CBF _A (mL/100 g/min)	52.8 ± 7.4* [§]	54.2 ± 8.6* [§]	63.1 ± 5.5 [§]	65.7 ± 5.6 [§]
Baseline V_0 (mL/100 g)	2.54 ± 0.73* [†]	1.37 ± 0.64* [†]	3.08 ± 1.03 [†]	1.75 ± 0.72 [†]
After ACZ V_0 (mL/100 g)	2.55 ± 0.87* [†]	1.39 ± 0.69* [†]	3.59 ± 0.76 [†]	2.13 ± 1.07 [†]
CVR (%)	17.4 ± 11.1*	17.0 ± 12.3*	25.5 ± 9.6	25.7 ± 10.5
Delay (s)	2.81 ± 0.14*		2.66 ± 0.15	
CMRO ₂ (mL/100 g/min)	2.87 ± 0.31*		3.06 ± 0.32	
OEF (%)	50.7 ± 4.8*		45.9 ± 5.7	
CBV (mL/100 g)	3.91 ± 0.70*		3.59 ± 0.72	

ACZ acetazolamide, CBF_B baseline cerebral blood flow, CBF_A cerebral blood flow after ACZ; CMRO₂ cerebral metabolic rate of oxygen, OEF oxygen extraction fraction, CBV cerebral blood volume

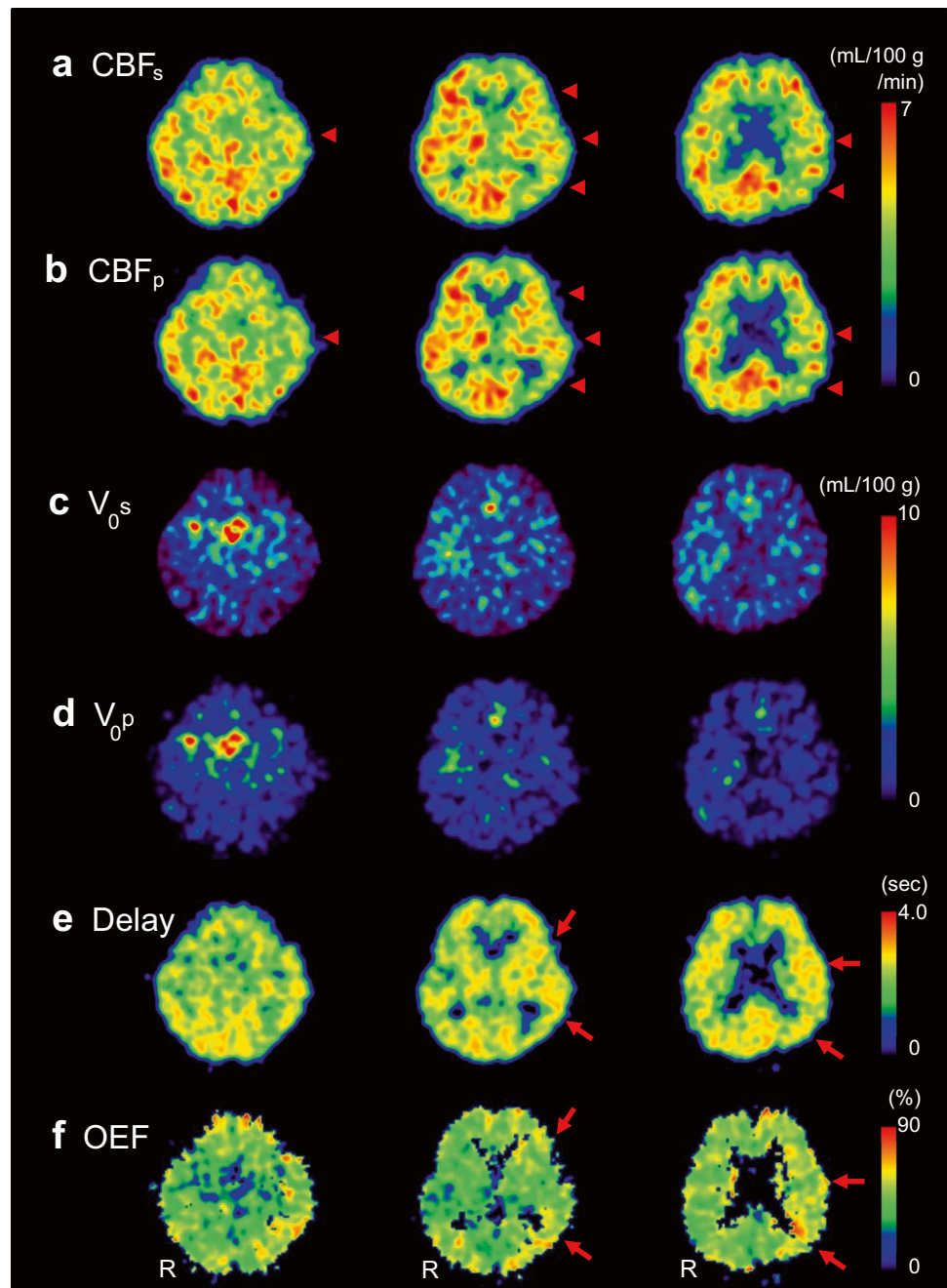
* $P < 0.05$ ipsi- vs. contra-lateral; [†] $P < 0.05$ slice-by-slice vs. pixel-by-pixel delay correction; [§] $P < 0.05$ before and after ACZ

curve fitting between C_a and TAC_{bp} for CBF and V_0 calculation is also given in Fig. 2 (dotted lines).

There were no differences in physiological data before and after the ACZ injection except for the arterial O_2 partial pressure (77.5 ± 9.4 vs. 86.5 ± 9.9 mmHg, $P < 0.001$). Mean values of hemodynamic parameters in the MCA region are given in Table 1. All parametric data showed significant differences between the two hemispheres; CBF, V_0 and $CMRO_2$ were significantly lower and CBV and OEF were significantly higher in the affected side compared with the contralateral hemisphere ($P < 0.05$). In the

comparison between pixel-by-pixel and slice-by-slice delay correction methods, V_0 values were significantly greater with the slice-by-slice than with the pixel-by-pixel correction method both before and after ACZ administration; however, CBF from the different correction methods did not show significant differences in both conditions. CVR values were significantly smaller in the ipsilateral side than the contralateral side for both pixel-by-pixel and slice-by-slice delay correction, and the two methods provided very close values. The delay image showed a significantly longer mean delay time in the affected hemisphere compared to

Fig. 3 Images from a representative case with left ICA stenosis (R at the *bottom* of each column shows *right* side of the patient): Baseline CBF images calculated by slice-by-slice **a** and pixel-by-pixel **b** delay correction show a CBF decrease in left MCA territory. *Arrowheads* indicate CBF decrease in the affected side. CBF values were very close between the two methods. *Baseline* V_0 images obtained by slice-by-slice **c** and pixel-by-pixel **d** delay correction show a significant difference in quantitative values between the two methods (2.08 vs. 1.27 mL/100 g in the global V_0 mean). Asymmetry indexes (% difference between the hemispheres) were 78 and 72% for slice-by-slice and pixel-by-pixel methods, respectively. A delay image **e** from the pixel-by-pixel method shows a longer delay time in the left hemisphere in accordance with the OEF elevation (**f**) (*arrows*)



that in the contralateral side (2.81 ± 0.14 s vs. 2.66 ± 0.15 s, $P < 0.05$). The asymmetry indices for the average delay times of the ipsi- to the contra-lateral hemispheres were in the range of 1.00–1.13.

Parametric images of a representative case of left ICA stenosis are given in Fig. 3. CBF images with pixel-by-pixel delay correction (Fig. 3b) show similar cortical regional values to those from slice-by-slice delay correction (Fig. 3a). V_0 images show significantly different quantitative values in the whole brain between the two delay correction methods (Fig. 3c, d). The delay image (Fig. 3e) shows the laterality of tracer arrival to be slightly longer in the affected left side (arrows) than in the contralateral side. The OEF image shows an ipsilateral increase compared with the contralateral side (Fig. 3f).

Figure 4 shows a pixelwise comparison between the two delay correction methods of pixel-by-pixel and slice-by-slice, in which CBF pixel values from the latter method were overestimated in the lower range although CBF values around 35 (mL/100 g/min) or higher showed a good correlation between the two methods. In contrast, V_0 pixel values from the slice-by-slice delay correction method were overestimated in the whole brain compared with the pixel-by-pixel correction.

Figure 5 shows analyses of the effects of estimation error in the delay time correction on CBF and V_0 values (time-shift simulation of the arterial input function from the true input function). A negative time shift indicates a delayed tracer arrival compared to the true input function at the local brain region, and a positive shift represents an advanced tracer arrival. Both parameters showed greater estimation errors in the longer time shift from the true input function; however, the error range in CBF was significantly smaller than the estimation errors observed in V_0 calculation. Smaller parametric values tended to show greater errors in error estimation of delay time in both parameters.

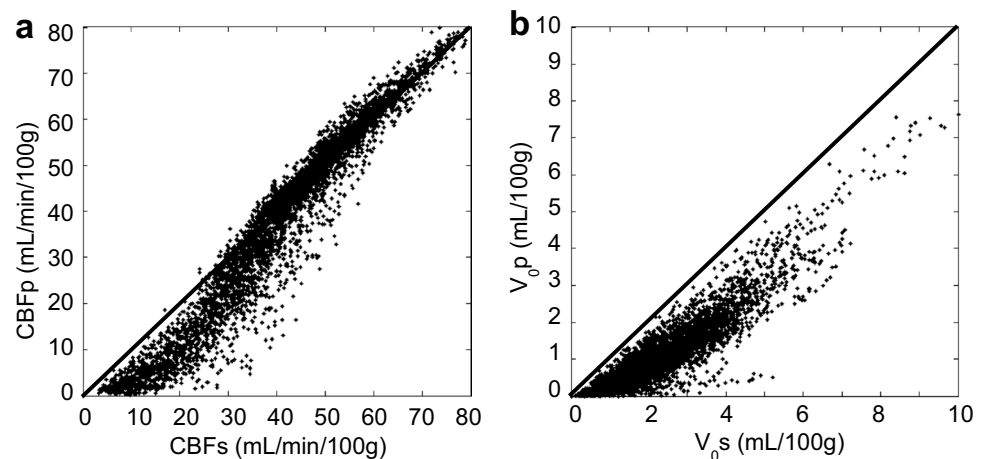
Figure 6 shows a representative case with left ICA occlusion, whose PET results significantly affected a treatment decision. Although the ^{15}O -PET study showed a slight decrease in baseline CBF in the MCA territory (Fig. 6d), no significant OEF increase was observed in the affected region (Fig. 6c). The ACZ challenge test showed a significant decrease in CVR (Fig. 6e), but baseline CBF did not decrease significantly, and the results indicated stage I hemodynamic impairment. The cerebral perfusion pressure (CPP) image calculated from CBF/V_0 showed a significant decrease after ACZ administration in left MCA territory (Fig. 6f, g), which indicated significant hemodynamic impairment. The patient underwent EC-IC bypass surgery because of the PET results and his symptoms of TIA.

Figure 7 shows the relationships of hemodynamic parameters obtained from this study. Although CBF did not show a correlation with delay time, CVR_p and OEF had significant negative (a: $r = -0.37$) and positive (b: $r = 0.37$) correlations with delay time, respectively ($P < 0.05$). The difference of delay time between the contralateral to the ipsilateral hemisphere showed a significant correlation with CVR_p as well (c: $r = -0.47$, $P < 0.05$). If we calculate cerebral perfusion pressure (CPP) with an equation of CBF/V_0 , CPP_p showed a good correlation with CBF linearly ($r = 0.39$, $P < 0.05$) or rather better in a logarithmic function (d: $r = 0.43$, $P < 0.01$). In contrast, V_0 and CBV did not show a significant correlation ($r = 0.24$).

Discussion

In the present study, a pixel-by-pixel delay time estimation for accurate correction was employed to calculate precise CBF and V_0 images. The mean values of cortical CBF were not significantly different between the methods and the scatter plots showed a good correlation in the moderate to high perfusion range although the slice-by-slice correction

Fig. 4 Pixelwise comparison of baseline CBF **a** and V_0 **b** between the methods of slice-by-slice (CBFs and V_0s) and pixel-by-pixel (CBFp and V_0p) delay correction. Scatter plots were obtained from pixel values of a representative image slice



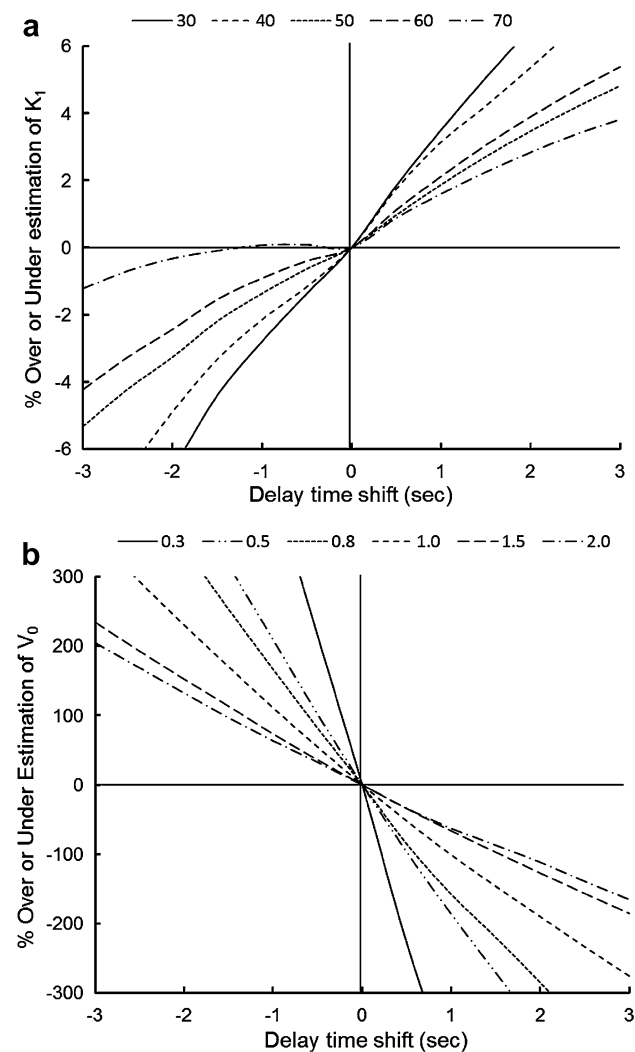


Fig. 5 Results from error analyses assessed for effects of delay time shift on CBF **a** and V_0 **b** values. A *negative* time shift assumes a delayed tracer arrival at the local brain region compared with the true input function, and a *positive* shift indicates an advanced tracer arrival. *Different lines* show various regional values of CBF (mL/min/100 g) and V_0 (mL/100 g) as given at the *top* of the graphs

method overestimated CBF values in the hypoperfused regions. Since the brain hypoperfused regions should have a longer delay time shift and errors were greater compared with the normal and high blood flow regions, CBF in those regions would have been overestimated in the slice-by-slice method (Figs. 5, 7). This result is important in a clinical setting because the hypoperfused regions are the target for hemodynamics evaluation and OEF increase due to CBF reduction should be the high risk region of hemodynamic infarction [24]. The ACZ challenge test with the perfusion SPECT or PET study is also useful for evaluating hemodynamic impairment in CVD patients, and it is used as an indication for EC-IC bypass surgery and other

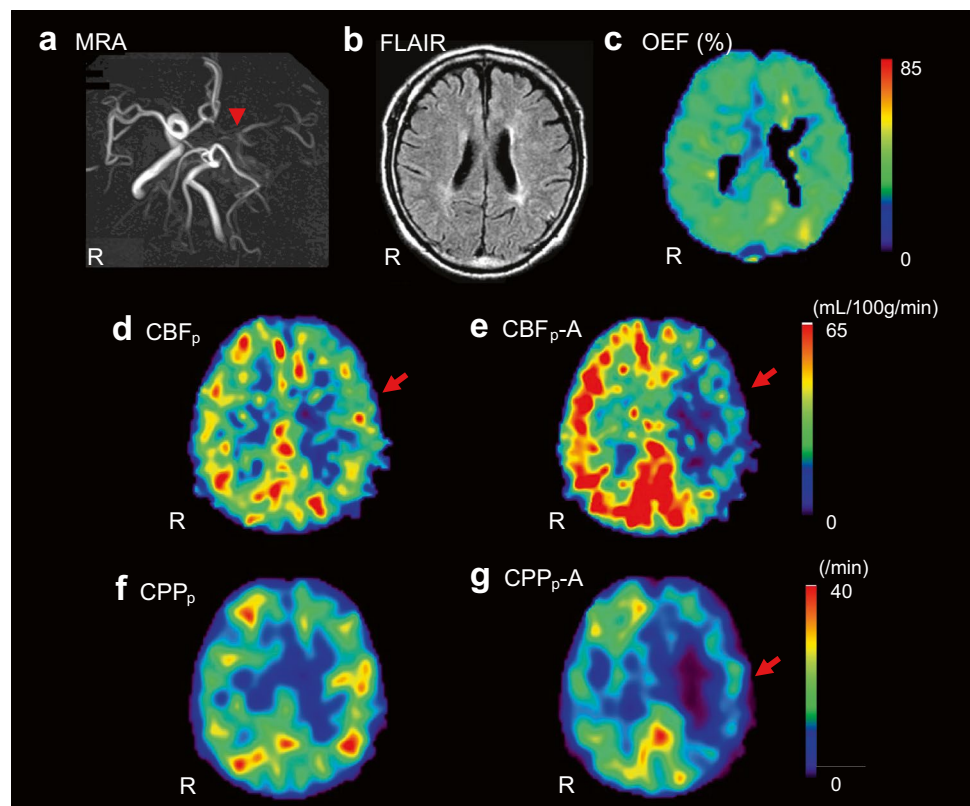
neurosurgical treatments in Japan [25, 26]. In both studies, precise measurement of CBF is very important.

V_0 values, however, showed significant difference between the two methods in the whole V_0 range of the brain because a slight shift of delay time estimation results in significant calculation errors [7]. The pixelwise delay for each brain location from TAC_{a2} was estimated in a narrow range of 0–4 s, which reduced the image calculation time compared with direct pixel-by-pixel delay estimation from the TAC_{a1} , and provided an accurate delay time for V_0 calculation. This delay of tracer arrival time from the ICA was almost identical to that in a previous study [9]. Direct delay estimation of TAC_{bp} from TAC_{a1} provided a greater range of delay between –5 s to more than 10 s depending on sclerotic and stenotic changes in the arteries of the blood sampling site and the local brain compared with our two-step correction method. The two-step method can avoid the effect of sclerotic changes in the brachial artery by adjusting TAC_{a1} to TAC_{CA} at first. Furthermore, the advantage of the pixel-by-pixel delay estimation is that it produces a delay time image which is a similar parameter to time-to-peak or arterial transit-time in MR perfusion studies, that would be beneficial information for the assessment of hemodynamic status in CVD patients. Because the delay time was correlated with OEF and CVR (Fig. 7), it may be able to estimate OEF elevation and CVR reduction without a $^{15}O_2$ scan or the ACZ challenge test. If the image derived input function method with ^{15}O -water PET is established, the delay image might be beneficial as one of the screening tools.

Previous studies reported that CBF values are sensitive to errors in delay time estimation, where a positive delay time shift shows overestimation and a negative shift underestimates CBF values [7, 9, 27]. We also observed similar estimation errors from the error analyses (Fig. 5a). The percent change in CBF values of less than 7% in the range of –2 to 2 s shift, which is consistent with the report by Iida et al. [9], seems small enough and acceptable. In the present study, the difference of CBF values between slice-by-slice and pixel-by-pixel delay correction was less than 4% in the cortical region, and the difference was not significant in statistical analysis. However, significantly longer delay times in the severely affected brain regions may induce significant errors in the slice-by-slice correction. Our two-step method with the positive delay time shift (0–4 s) seems more robust in CBF measurement with negligible errors compared to the slice-by-slice direct correction method.

In contrast, V_0 values seem to be more vulnerable to errors in delay estimation than in CBF [7]. The error range is not negligible because only a 1 s time shift may cause 50–200% difference in the V_0 range of 0.5–2.0 (mL/100 g) (Fig. 5b). The significant overestimation of V_0 values with a small error of delay estimation in the slice-by-slice method

Fig. 6 A representative case from this study. The patient had left ICA occlusion on MRA (a). Arrowhead shows the occlusion of ICA. MRI FLAIR image showed no significant ischemic region in the MCA territory (b). Although OEF image showed no significant increase in the left cerebral hemisphere (c), baseline CBF_p showed a tendency of decrease in the MCA territory (d). ACZ challenge test showed significant decrease in CBF_p (e) and CPP_p (f baseline, g after ACZ) in the affected region. The study indicated significant hemodynamic impairment because of the significant decrease in CVR and CPP, and the patient underwent EC–IC bypass surgery. CBF_{p-A} and CPP_{p-A} means pixel-by-pixel calculated CBF and CPP after ACZ. R on each panel represents right side of the patient. Red arrows show affected side of MCA territory



may have a severe effect in a clinical setting, which confirms the necessity of pixel-by-pixel delay correction. The V_0 apparently reflects the arterial-to-capillary blood volume, which is different from CBV including venous volume [7, 11, 28]. To evaluate cerebral perfusion pressure (CPP) from PET parameters, CBF/V_0 would be more appropriate than CBF/CBV values [14, 28], and images with precise regional values of V_0 offer beneficial information for the assessment of hemodynamics of CVD. The high temporal resolution (0.1 s) for delay time estimation between TAC_{a2} and C_{bp} in the present study is preferable for this precise estimation of PET parameters because different time steps of 0.1 and 1.0 s for delay estimation showed differences in delay time as well as V_0 values (Fig. 8). The residuals for the fittings with 1.0, 0.1 and 0.01 s steps were almost the same and CBF values did not show differences; however, the 1.0 s step delay time estimation provided significantly different V_0 values not only in the affected side, but also in the contralateral side compared with those of 0.1 or 0.01 s steps (data not shown). Because the different time steps of 0.1 and 0.01 s did not lead to differences in the results of delay, CBF and V_0 , we decided to use 0.1 s steps for delay time estimation. The calculation time of the delay estimation was not much affected by difference in the temporal resolution (step size). However, least-squares fitting for CBF and V_0 calculation using Eq. 3 is still time consuming even after recent improvements in computer power. The

weighted integration method reduces calculation time significantly as previously reported [6, 7, 29].

Regional CVR_p , which reflects the vasodilatory capacity, showed a significant correlation with delay time and asymmetry of delay (Fig. 7a, c). The negative correlation represents a longer tracer arrival time in the severely affected region, which is consistent with impaired hemodynamic change in the area. Although the means of delay time in the ipsi- and contra-lateral hemispheres showed only 0.15 s difference (Table 1), a mean value is often blurred by the mixing of significant and insignificant results, and the statistical analysis showed that the difference was significant. Parameters of oxygen metabolism measured by ^{15}O -gas PET could be compared with the new parameters in the present study because this is a retrospective study to propose the better analyses of patients' hemodynamic conditions using ^{15}O -water PET. OEF showed a significant correlation with delay time (Fig. 7b), indicating that delay time is closely correlated with hemodynamic impairment. The lower range of CPP showed a positive correlation with CBF although CBF tended to reach a plateau value in higher CPP. This correlation is also consistent with the theory of hemodynamic changes [14, 15, 30], as we previously reported the importance of precise estimation of V_0 for the CPP evaluation [28].

In the present study, the pixel-by-pixel calculation estimated V_0 in the contralateral hemisphere to be about 49%

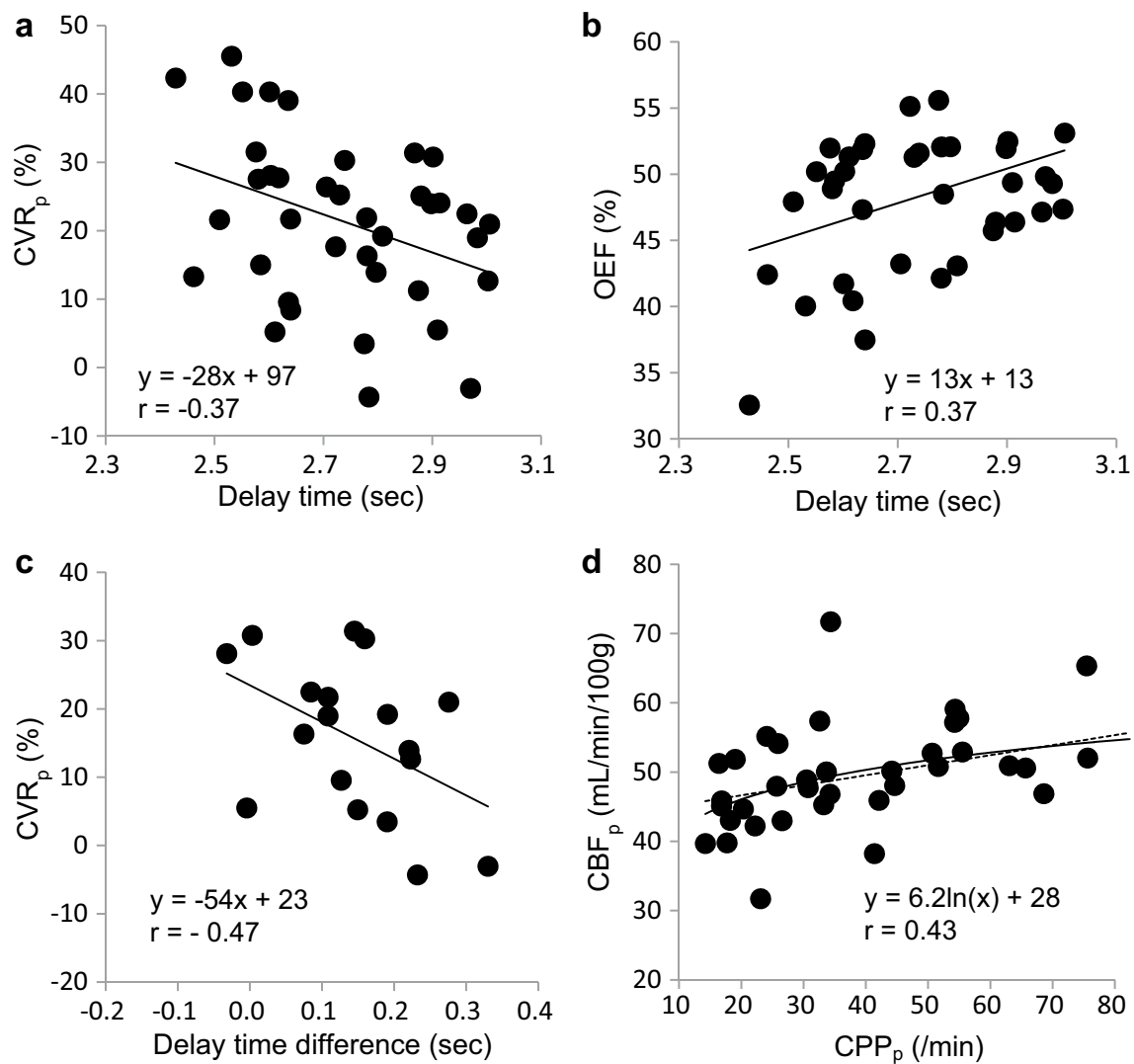


Fig. 7 Different hemodynamic parameters were plotted from pixel-by-pixel delay estimation. The best fit regression line for correlation analysis was selected for each graph. **a** Delay time vs. CVR_p ($P < 0.05$), **b** Delay vs. OEF, ($P < 0.05$), **c** Delay time difference

between contra- and ipsi-lateral hemisphere vs. CVR_p , ($P < 0.05$), **d** arterial cerebral perfusion pressure (CPP_p) obtained from CBF/V_{0p} vs. CBF_p ($P < 0.01$). Dashed line shows linear regression ($y = 0.15x + 43.7$, $r = 0.39$, $P < 0.05$)

of CBV, which is close to the values in the previous reports (about 20–40%) [31, 32]. However, the slice-by-slice delay correction estimated contralateral V_0 to be about 87% of CBV, which is greater than our previous studies showing V_0 values of less than 60% of CBV [11, 28]. Although the difference in the initial frame time (5 s in the previous studies) may have provided greater V_0 values in the slice-by-slice calculation method, the initial slope at tracer arrival was estimated better in 2-sec than in 5-s frames, especially when obtaining the TAC_{CA} . The coefficient of variation (COV) values were calculated from ROIs drawn on each cerebral hemisphere of the patients. CBF images showed no difference in COV (0.18 ± 0.02 for both calculation methods), and V_0 images showed 0.37 ± 0.07 and 0.50 ± 0.11 for

the slice-by-slice and pixel-by-pixel methods, respectively. This result indicates that the V_0 image was noisier in the latter method than in the former one, and improvement of image quality may be needed for V_0 evaluation.

Since the patients enrolled in this study had only minor symptoms and half of them were asymptomatic, we might have seen different results from severely affected cerebral circulation in symptomatic patients. However, a tendency of hemodynamic impairment in the chronic phase of CVD was observed in the present study, suggesting that this method for precise estimation of delay time correction would be ideal for the assessment of CVD caused by stenooclusive lesions in the major cerebral arteries. Baseline V_0 tended to show smaller values in the ipsilateral side compared with the contralateral side (Table 1),

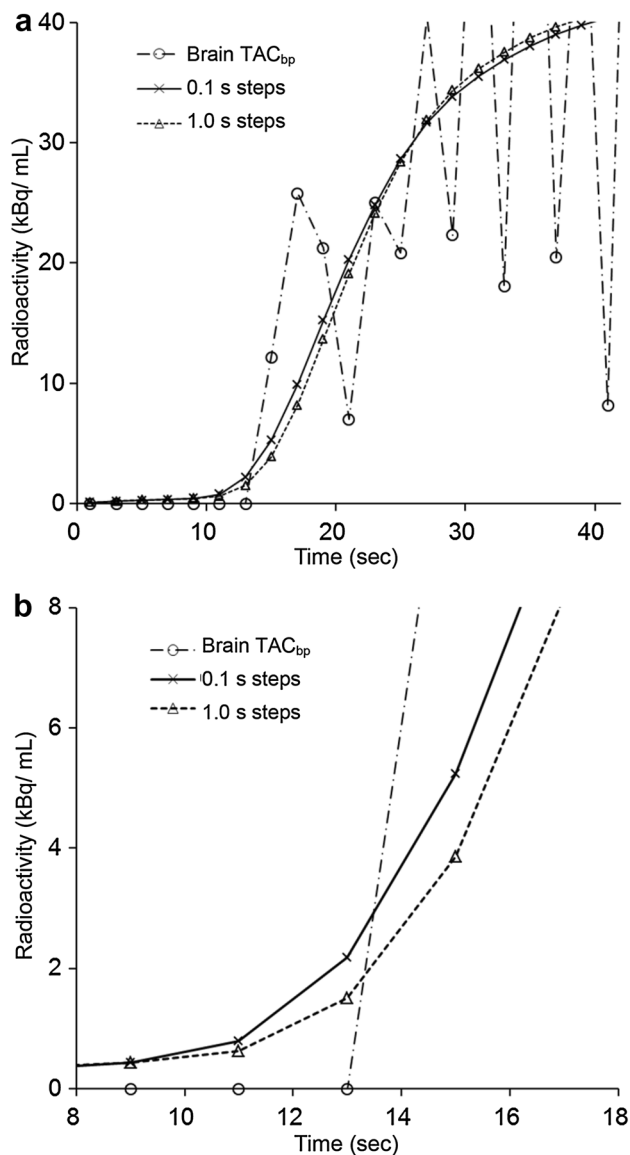


Fig. 8 Representative curves of TAC_{bp} and TAC_{a2} after fitting using the least-squares method for delay estimation (**a**) and zoom of the graph between 8 and 18 s (**b**). 0.1 s steps showed a better fitting curve (solid line) than 1.0 s steps (dotted line) and delay times from these fittings were estimated to be 1.6 and 2.0 s for 0.1 and 1.0 s steps, respectively. These delay times estimated quantitative values of this voxel to be 34.1 and 33.5 (mL/100 g/min) for CBF and 0.9 and 1.4 (mL/100 g) for V_0 , respectively. The statistical analysis showed that CBF_p was not different in cortical values, but V_0 p was significantly different for both hemispheres

and the result was similar to the previous works [28, 33]. In the chronic phase of CVD, the arteriole-to-capillary part of vessels may not necessarily show vasodilatory change, and increase in CBV is assumed to be caused mainly by increase in venous volume. In the present study, only a few cases were in the stage of misery perfusion assessed by a significant OEF increase, and these

patients also did not show significant increase in ipsilateral V_0 . Microvascular impairment in cerebral ischemic change may cause capillary collapse in the chronic phase of CVD [34].

Conclusion

The precise estimation of hemodynamic parameters such as CBF and V_0 using the new method should be ideal and beneficial for clinical use. Pixel-by-pixel delay estimation also provides a new image of delay time that should provide useful information for the clinical assessment of CVD.

Acknowledgements The authors thank the staff of the Biomedical Imaging Research Center and doctors in the Department of Neurosurgery, University of Fukui for technical and clinical support. This study was partly funded by a Grant-in-Aid for Scientific Research from the Japan Society for the Promotion of Science (15K15453).

Compliance with ethical standards

Financial support This study was partly funded by a Grant-in-Aid for Scientific Research from the Japan Society for the Promotion of Science (15K15453).

Open Access This article is distributed under the terms of the Creative Commons Attribution 4.0 International License (<http://creativecommons.org/licenses/by/4.0/>), which permits unrestricted use, distribution, and reproduction in any medium, provided you give appropriate credit to the original author(s) and the source, provide a link to the Creative Commons license, and indicate if changes were made.

References

1. Frackowiak RS, Lenzi GL, Jones T, Heather JD. Quantitative measurement of regional cerebral blood flow and oxygen metabolism in man using ^{15}O and positron emission tomography: theory, procedure, and normal values. *J Comput Assist Tomogr.* 1980;4:727–36.
2. Herscovitch P, Markham J, Raichle ME. Brain blood flow measured with intravenous H_2^{15}O . I. Theory and error analysis. *J Nucl Med.* 1983;24:782–9.
3. Raichle ME, Martin WRW, Herscovitch P, Mintun MA, Markham J. Brain blood flow measured with intravenous H_2^{15}O : II. Implementation and validation. *J Nucl Med.* 1983;24:790–8.
4. Kanno I, Iida H, Miura S, Murakami M, Takahashi K, Sasaki H, et al. A system for cerebral blood flow measurement using an H_2^{15}O autoradiographic method and positron emission tomography. *J Cereb Blood Flow Metab.* 1987;7:143–53.
5. Gambhir SS, Huang SC, Hawkins RA, Phelps ME. A study of the single compartment tracer kinetic model for the measurement of local cerebral blood flow using ^{15}O water and positron emission tomography. *J Cereb Blood Flow Metab.* 1987;7:13–20.
6. Ohta S, Meyer E, Thompson CJ, Gjedde A. Oxygen consumption of the living human brain measured after a single

- inhalation of positron emitting oxygen. *J Cereb Blood Flow Metab.* 1992;12:179–92.
7. Ohta S, Meyer E, Fujita H, Reutens DC, Evans A, Gjedde A. Cerebral [^{15}O]water clearance in humans determined by PET: I. Theory and normal values. *J Cereb Blood Flow Metab.* 1996;16:765–80.
 8. Toussaint PJ, Meyer E. A sensitivity analysis of model parameters in dynamic blood flow studies using H_2^{15}O and PET. In: Myers R, Cunningham V, Bailey D, Jones T, editors. *Quantification of brain function using PET.* San Diego: Academic Press; 1996. pp. 196–200.
 9. Iida H, Higano S, Tomura N, Shishido F, Kanno I, Miura S, et al. Evaluation of regional differences of tracer appearance time in cerebral tissues using [^{15}O]water and dynamic positron emission tomography. *J Cereb Blood Flow Metab.* 1988;8:285–8.
 10. Iida H, Kanno I, Miura S, Murakami M, Takahashi K, Uemura K. A determination of the regional brain/blood partition coefficient of water using dynamic positron emission tomography. *J Cereb Blood Flow Metab.* 1989;9:874–85.
 11. Okazawa H, Yamauchi H, Sugimoto K, Takahashi M, Toyoda H, Kishibe Y, et al. Quantitative comparison of the bolus and steady-state methods for measurement of cerebral perfusion and oxygen metabolism: Positron emission tomography study using ^{15}O -Gas and Water. *J Cereb Blood Flow Metab.* 2001;21:793–803.
 12. Okazawa H, Vafaei M. Effect of vascular radioactivity on regional values of cerebral blood flow evaluation of methods for H_2^{15}O PET to distinguish cerebral perfusion from blood volume. *J Nucl Med.* 2001;42:1032–9.
 13. Iida H, Law I, Pakkenberg B, Krarup-Hansen A, Eberl S, Holm S, et al. Quantitation of regional cerebral blood flow corrected for partial volume effect using O-15 water and PET: I. Theory, error analysis, and stereologic comparison. *J Cereb Blood Flow Metab.* 2000;20:1237–51.
 14. Okazawa H, Kudo T. Clinical impact of hemodynamic parameter measurement for cerebrovascular disease using positron emission tomography and ^{15}O -labeled tracers. *Ann Nucl Med.* 2009;23:217–27.
 15. Powers WJ, Zazulia AR. PET in cerebrovascular disease. *PET Clin.* 2010;5(1):83106.
 16. DeGrado TR, Turkington TG, Williams JJ, Stearns CW, Hoffman JM, Coleman RE. Performance characteristics of a whole-body PET scanner. *J Nucl Med.* 1994;35:1398–1306.
 17. Isozaki M, Kiyono Y, Arai Y, Kudo T, Mori T, Maruyama R, et al. Feasibility of ^{62}Cu -ATSM PET for evaluation of brain ischemia and misery perfusion in patients with cerebrovascular disease. *Eur J Nucl Med Mol Imaging.* 2011;38:1075–82.
 18. Okazawa H, Tsuchida T, Kobayashi M, Arai Y, Pagani M, Isozaki M, et al. Can reductions in baseline CBF and vasoreactivity detect misery perfusion in chronic cerebrovascular disease? *Eur J Nucl Med Mol Imaging.* 2007;34:121–9.
 19. Mintun MA, Raichle ME, Martin WRW, Herscovitch P. Brain oxygen utilization measured with 0–15 radiotracers and positron emission tomography. *J Nucl Med.* 1984;25:177–87.
 20. Okazawa H, Kishibe Y, Sugimoto K, Takahashi M, Yamauchi H. Delay and dispersion correction for a new coincidental radioactivity detector, pico-count, in quantitative PET studies. In: Senda M, Kimura Y, Herscovitch P, editors. *Brain imaging using PET.* San Diego, CA: Academic Press; 2002. pp. 15–21.
 21. Vafaei M, Murase K, Gjedde A, Meyer E. Dispersion correction for automatic sampling of O-15-labeled H_2O and red blood cells. In: Myers R, Cunningham V, Bailey D, Jones T, editors. *Quantification of brain function using PET.* San Diego: Academic Press; 1996. pp. 72–5.
 22. Meyer E. Simultaneous correction for tracer arrival delay and dispersion in CBF measurements by the H_2^{15}O autoradiographic method and dynamic PET. *J Nucl Med.* 1989;30:1069–78.
 23. Iida H, Kanno I, Miura S, Murakami M, Takahashi K, Uemura K. Error analysis of a quantitative cerebral blood flow measurement using H_2^{15}O autoradiography and positron emission tomography, with respect to the dispersion of the input function. *J Cereb Blood Flow Metab.* 1986;6:536–45.
 24. Yamauchi H, Higashi T, Kagawa S, Nishii R, Kudo T, Sugimoto K, et al. Is misery perfusion still a predictor of stroke in symptomatic major cerebral artery disease? *Brain.* 2012;135:2515–26.
 25. Ogasawara K, Ogawa A, Yoshimoto T. Cerebrovascular reactivity to acetazolamide and outcome in patients with symptomatic internal carotid or middle cerebral artery occlusion: a xenon-133 single-photon emission computed tomography study. *Stroke.* 2002;33:1857–62.
 26. Kuroda S, Houkin K, Kamiyama H, Mitsumori K, Iwasaki Y, Abe H. Long-term prognosis of medically treated patients with internal carotid or middle cerebral artery occlusion: can acetazolamide test predict it? *Stroke.* 2001;32:2110–6.
 27. Kudomi N, Maeda Y, Sasakawa Y, Monden T, Yamamoto Y, Kawai N, et al. Imaging of the appearance time of cerebral blood using [^{15}O]H $_2\text{O}$ PET for the computation of correct CBF. *Eur J Nucl Med Mol Imaging Res.* 2013;3:41.
 28. Okazawa H, Yamauchi H, Toyoda H, Sugimoto K, Fujibayashi Y, Yonekura Y. Relationship between vasodilatation and cerebral blood flow increase in impaired hemodynamics: a PET study with the acetazolamide test in cerebrovascular disease. *J Nucl Med.* 2003;44:1875–83.
 29. Ito H, Iida H, Bloomfield PM, Murakami M, Inugami A, Kanno I, et al. Rapid calculation of regional cerebral blood flow and distribution volume using iodine-123-iodo-amphetamine and dynamic SPECT. *J Nucl Med.* 1995;36:531–6.
 30. Powers WJ. Cerebral hemodynamics in ischemic cerebrovascular disease. *Ann Neurol.* 1991;29:231–40.
 31. Ito H, Kanno I, Iida H, Hatazawa J, Shimosegawa E, Tamura H, Okudera T. Arterial fraction of cerebral blood volume in humans measured by positron emission tomography. *Ann Nucl Med.* 2001;15:111–6.
 32. Mellander S, Johansson B. Control of resistance, exchange, and capacitance functions in the peripheral circulation. *Pharmacol Rev.* 1968;20:117–96.
 33. Okazawa H, Yamauchi H, Sugimoto K, Takahashi M. Differences of vasodilatory capacity and changes in cerebral blood flow induced by acetazolamide in patients with cerebrovascular disease. *J Nucl Med.* 2003;44:1371–8.
 34. Taylor ZJ, Hui ES, Watson AN, et al. Microvascular basis for growth of small infarcts following occlusion of single penetrating arterioles in mouse cortex. *J Cereb Blood Flow Metab.* 2016;36:1357–73.